Highly stable noble metal nanoparticles dispersible in biocompatible solvents: synthesis of cationic phosphonium gold nanoparticles in water and DMSO

Yon Ju-Nam*[,†], Wanisa Abdussalam-Mohammed[†], Jesus J. Ojeda[‡]

[†]*Swansea University, College of Engineering, Engineering Central Building, Bay Campus, Crymlyn Burrows, Swansea, SA1 8EN, United Kingdom*

[‡]*Brunel University London, Institute of Materials and Manufacturing, Experimental Technique Centre, Uxbridge, UB8 3PH, United Kingdom*

**To whom correspondence should be addressed. E-mail: y.k.ju-nam@swansea.ac.uk*

Abstract

In this work, we report the synthesis of novel cationic phosphonium gold nanoparticles dispersible in water and dimethylsulfoxide (DMSO) for their potential use in biomedical applications. All the cationic-functionalising ligands currently reported in the literature are ammonium-based species. Here, the synthesis and characterisation of an alternative system, based on phosphonioalkylthiosulfate zwitterions and phosphonioalkylthioacetate were carried out. We have also demonstrated that our phosphonioalkylthiosulfate zwitterions readily disproportionate into phosphonioalkylthiolates *in situ* during the synthesis of gold nanoparticles produced by the borohydride reduction of gold (III) salts. The synthesis of the cationic gold nanoparticles using these phosphonium ligands were carried out in water and DMSO. UV-Visible spectroscopic and TEM studies have shown that the phosphonioalkylthiolates bind to the surface of gold nanoparticles which are typically around 10nm in diameter. The resulting cationic-functionalised gold nanoparticles are dispersible in aqueous medium and in DMSO, which is the only organic solvent approved by the U.S. Food and Drug Administration (FDA) for drug carrier tests. This indicates their potential future use in biological applications. This work shows the synthesis of a new family of phosphonium-

based ligands, which behave as cationic masked thiolate ligands in the functionalisation of gold nanoparticles. These highly stable colloidal cationic phosphonium gold nanoparticles dispersed in water and DMSO can offer a great opportunity for the design of novel biorecognition and drug delivery systems.

1. Introduction

The ability of modifying noble metal nanoparticles, such as gold nanoparticles with various organic thiolate ligands makes them versatile systems and opens a range of possibilities for their use as drug delivery systems,[1-3] and biosensing[4-6] applications. Even though the use of these nanoparticles in therapeutic purposes is promising, challenges still remain and when designing drug nanocarriers, the following considerations are usually taking into account: (i) possible drawbacks due to free drugs, (ii) tissue permeation and cellular uptake, and (iii) homogenous distribution within the target tissues and organs.[7-13] Therefore, for any biomedical application the main requirements are the affinity to aqueous media and compatibility with the immediate biological environment or appropriate receptor groups for sensing or diagnostic applications.

Ligands are introduced to the surface of the nanoparticle either to stabilise the particle and avoid uncontrolled aggregation, or to add functionality to the particle for biomolecular recognition, enhance transport and anchoring properties.[7] Recent studies have shown that the size, shape and surface charge of nanoparticles, in general, play crucial roles in their entry and subsequent access of nanoparticles into living cells.[6,13-16] For instance, cationic nanoparticles are more effective penetrating into mammalian cells than anionic nanoparticles.[17] Nanoparticle surface functionalisation plays an important role in the cellular uptake and producing cellular responses.[18,19] However, information published in the literature on how functionalised nanoparticle surface characteristics, such as aromaticity and

hydrophobicity, affect cellular internalisation processes is still unclear. Al-Hajaj et al. have shown that the functionalised quantum dots they produced with non-specified ligands were taken up by lipid host mediated endocytosis in human kidney and liver cells.[20] Designing and tailoring the surface of inorganic nanoparticles with suitable ligands may potentially offer long-term stability under a wide-range of conditions such as, high electrolyte concentration, a broad pH range, and biogenic or naturally occurring thiols.[3] Zhan et al. have shown that quantum dots modified with multidentate lipoic ligand containing a zwitterionic head group can be highly biocompatible nanomaterials,[21-22] making them attractive nanodevices for clinical *in vitro* and *in vivo* imaging applications.[23-25] More recently, Rotello et al. have studied the behaviour of gold nanoparticles with different hydrophobicities and the effect of surface functionality on hemolysis.[26] They observed a linear haemolytic behaviour with increasing hydrophobicity in the absence of serum media. McIntosh et al. synthesised gold nanoparticles capped with a mixture of octanethiol and 11-trimethylammonium-undecanethiol, and others functionalised with trimethylammonium cationic head groups on the surface can interact electrostatically and bind with the negatively charged phosphate backbone of 37mer duplex DNA.[27] As in these studies reported in the literature, the majority of the cationic species investigates and used are ammonium -based groups. Here in this work, we are proposing the use of cationic phosphonium-based groups as alternatives to the ammonium ones. The phosphonium groups can offer a range of advantages including the availability of a broad range of organic derivatives, which allows of designing and producing a wide variety of functionalised gold nanoparticles. Their ability of triphenylphosphonium head groups to travel across cell membranes is well-known.[28-30] There are also several studies on the use of phosphines and phosphine oxides to stabilise nanoparticles. However, there have been far fewer studies of the use of organophosphorus ligands.[31-33]

Additional to imparting specific functionalities to nanoparticles, their dispersion in water or any other biocompatible solvent is crucial for their use in biomedical or biological applications. Therefore, water should be the primary solvent to be used to disperse functionalised nanoparticles. However, in many cases, the ligands used to protect and provide functionality to nanoparticles, and the corresponding nanomaterials produced are not soluble or dispersible in water. It would be highly beneficial to have a range of other biocompatible solvents. One potential alternative to water may be dimethyl sulfoxide (DMSO). According to the FDA, DMSO is a solvent derived from wood, which has been the subject of considerable interest for its potential as a drug. At present, the only human use for which DMSO has been approved is for interstitial cystitis, a bladder condition. DMSO is also known as a "carrier" chemical, it could deliver substances into the bloodstream through the skin.[34] For all the reasons outlined here, DMSO was a chosen solvent to synthesise and disperse our nanoparticles.

Here in this paper we are reporting for the first time the syntheses cationic gold nanoparticles by reducing gold (III) salt in the presence of our cationic phosphonium ligands in DMSO. We also describe the synthesis of a new cationic phosphonium ligand, tri(*p*-tolyl)phosphoniopropylthiosulfate zwitterion used to functionalise the gold nanoparticle surface in DMSO. Two previously reported phosphonium ligands, triphenylphosphoniopropylthiosulfate zwitterion[35] and (3-thioacetylpropyl)triphenylphosphonium bromide,[36] were used for this work to produce the cationic phosphonium gold nanoparticles in DMSO and comparison purposes with the new ligand synthesised, tri(*p*-tolyl)phosphoniopropylthiosulfate.

2. Materials and Methods

(a) General

All chemicals and solvents were purchased from Sigma-Aldrich and Fisher Scientific Ltd. For the characterisation of the ligands and functionalised gold nanoparticles several analytical techniques were used. TLC, ATR-FTIR, NMR, ESI-MS techniques were employed to characterise the phosphonium containing ligands. UV-Visible spectroscopy and TEM were used to characterise and obtain the size of the cationic phosphonium gold nanoparticles. The stability of the colloidal gold nanoparticle solutions were monitored using UV-Visible technique.

Thin Layer Chromatography (TLC): Analytical thin layer chromatography was carried out on Merck silica gel 60 F254 plates by using mixtures of methanol: dichloromethane (DCM) as eluent system.

Attenuated Total Reflectance – Fourier Transform Infrared (**ATR-FTIR) Spectroscopy**: IR spectra acquisition was performed on solid samples using a Nicolet 5700 FT-IR spectrometer equipped with Omnic software (version 7.1) and a Smart Omni-Sampler (ATR cell with single reflectance germanium crystal). Each recorded spectrum is the average of 32 scans with a spectral resolution of 4 cm^{-1} from 400 to 4000 cm^{-1} on a dried sample, with a background spectrum recorded before each analysis. Spectra were measured and analysed and fitted using Origin software (Version 7.5) equipped with Peak-Fitting Module (PFM).

Nuclear Magnetic Resonance Spectroscopy (NMR): ^{1}H NMR spectra were acquired on a JEOL 400MHz spectrometer. Data are reported as follows: *s*, singlet; *d*, doublet; *t*, triplet; *q*, quartet; *m*, multiplet. Appropriate solvents such as dimethylsulfoxide, chloroform, diethyl

ether were used to dissolve the samples to a concentration of 15 to 40 mg ml^{-1} for ^{1}H experiments.

Electrospray Ionisation – Mass Spectrometry (ESI-MS): ESI-MS analyses were generally performed on the Orbitrap XL using nano- electrospray in positive or negative ionisation mode. Orbitrap XL High resolution instrument gives accurate mass measurement over the full mass range in electrospray resolution: up to 100,000 (FWHM). Mass Range: m/z 50–2000 or m/z 200–4000. Mass Accuracy: <3 ppm RMS with external calibration; <2 ppm RMS with internal calibration.

All samples were initially solvated in 250µl of DCM before approximately 10µl of the solutions were added to 1ml of methanol with NH_4OAc. A portion of these samples were added to a 96 well plate to be analysed by positive nano-electrospray.

Ultraviolet-Visible Absorption Spectroscopy (UV-visible): UV-visible spectra were obtained on a HITACHI U-2900 spectrophotometer with double beam principle system with data recording using Vision software version on Windows XP/2000. Samples were analysed in a UV-quartz cuvette of a 1 cm optical path. Appropriate dilutions to the original samples were carried out using either water or DMSO.

Transmission Electron Microscopy (TEM): A JEOL2100 field emission gun transmission electron microscope (FEG TEM) set at 100 KV was used for the analyses of the particles and obtained the TEM micrographs. Size distribution was obtained by counting and measuring over 150 gold nanoparticles. Deposition method was used to prepare the samples for TEM analyses. A drop of a diluted colloidal solution of the functionalised gold nanoparticles was placed and suspended on a Holey carbon coated copper grid. Then the grids were left to dry at room temperature.

(b) Synthesis of Cationic Phosphonium Ligands

The tri(*p*-tolyl)phosphoniopropylthiosulfate zwitterion synthesis and characterisation are reported for the first time in this work. The syntheses of the triphenylphosphoniopropylthiosulfate zwitterion and ω-thioacetylpropylphosphonium salt were carried out following previously reported methods.[35,36] The synthetic protocols used to produce the three ligands are outlined in this section.

Synthesis of tri(*p*-tolyl)phosphoniopropylthiosulfate zwitterion

The synthesis of the tri(*p*-tolyl)phosphoniopropylthiosulfate zwitterion was carried out following the reactions showed in **Scheme 1**. In a round bottom flask with a reflux condenser a mixture of tri(*p*-tolyl)phosphine **(1)** (3.8mmol) with approximately bromo-propanol (15 mmol) were refluxed for five hours in acetonitrile (0.024 mmol) and the solid precipitate was collected and recrystallized from ethanol (Reaction 1, Scheme1). The yield was 70%. The resulting salt **(2)** was dissolved in hydrobromic acid (0.18 mmol, 10 ml) (48%) in a round bottom under reflux five hours (Reaction 2, Scheme 1). The reaction mixture was left to cool down, the compound appeared as yellow oil **(3)**. In order to prepare the tri-*p*-tolylphosphoniopropylthiosulfate zwitterion **(4)**, a mixture of ω-bromopropyl-tri(*p*-tolyl)phosphonium bromide **(3)** (1 mmol) and sodium thiosulfate (1.5 mmol) were refluxed for five hours in aqueous ethanol (1:1, 10ml) (Reaction 3, Scheme 1). TLC was used in order to follow the progress of the reaction by using 20%:80% methanol:DCM as mobile phase. All compounds were purified further by liquid-liquid extraction of the reaction mixture using DCM and by trituration with dry diethyl ether.

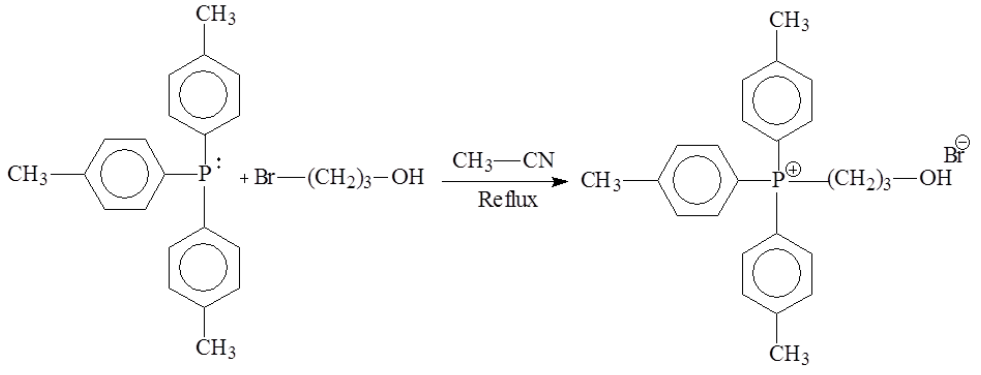

(1) (2)

Reaction 1

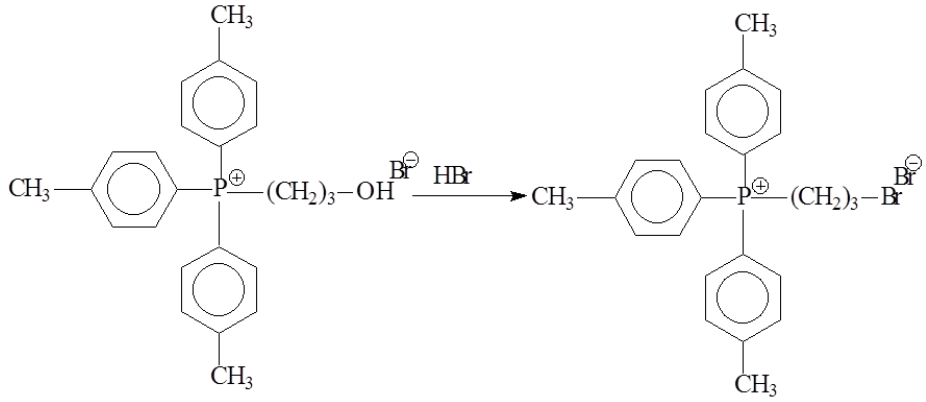

(2) (3)

Reaction 2

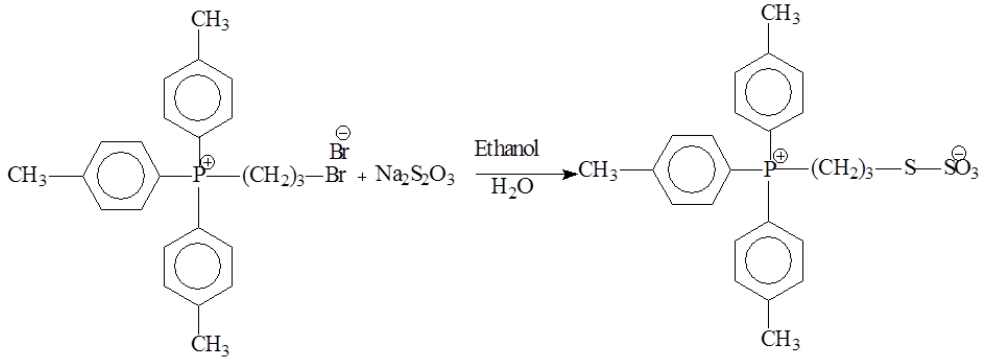

(3) (4)

Reaction 3

Scheme 1: Synthesis of tri(*p*-tolyl)phosphoniopropylthiosulfate zwitterion (4)

Synthesis of triphenylphosphoniopropylthiosulfate

In order to obtain the triphenylphosphoniopropylthiosulfate zwiterion,[35] three main chemical reactions were carried out. The first stage involved the synthesis of the hydorxylpropylphosphonium salt and this was generated by a quaternation reaction of triphenylphosphine (4 mmol) and the corresponding bromo-propanol (15 mmol) in acetonitrile under reflux for four to five hours. The resulting salt was dissolved in hydrobromic acid (48%) and reaction was carried out under reflux for five hours to obtain the ω-bromopropyltriphenylphosphonium bromide salt. The latter (1 mmol) then was treated with sodium thiosulfate (1.5 mmol) in ethanol/water under reflux for five hours in order to produce the phosphoniopropylthiosulfate zwitterion. Progress of all reactions were monitored by TLC using methanol:dichloromethane 1:4 ratio as the mobile phase. All the compounds were purified by dichloromethane extraction and re-crystallisation using diethyl ether.

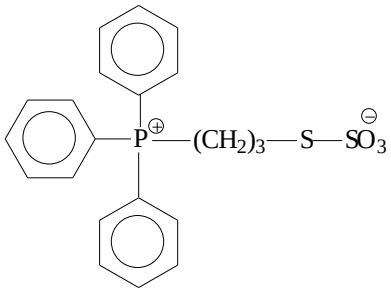

Triphenylphosphoniopropylthiosulfate zwitterion

Synthesis of (3-thioacetylpropyl)triphenylphosphonium bromide

In order to obtain the (3-thioacetylpropyl)triphenylphosphonium bromide, hydroxypropylphosphonium and ω-bromopropyltriphenylphosphonium bromide salts were also synthesised as described in the synthesis of triphenylphosphoniopropylthiosulfate zwitterion.[35,36] Once the bromide salt (2mmol) was produced, this was reacted with potassium thioacetate (3 mmol) in a mixture of ethanol/water. The progress of the reaction was followed by TLC using a mobile phase of methanol:dichloromethane in 1:4 ratio. The (3-

thioacetylpropyl)triphenylphosphonium bromide was isolated and purified by liquid-liquid extraction using DCM as the extracting solvent, and re-crystallisation of the bromide salt using diethyl ether.

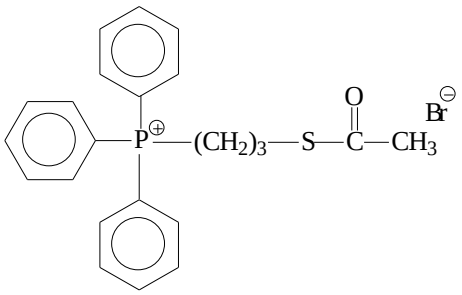

(3-Thioacetylpropyl)triphenylphosphonium bromide

(c) Synthesis of cationic phosphonium gold nanoparticles in DMSO and water

The method for the synthesis of colloidal cationic phosphonium gold nanoparticles in DMSO is reported for the first time in this work. These nanoparticles were obtained by a reduction of the gold salt in the presence of protecting ligands in DMSO. Colloidal cationic phosphonium gold nanoparticle solutions in water were also prepared for comparison purposes, following the principles involved in the method developed by Brust and Schifrin, a two-phase liquid-liquid system.[35] Variations were made to this protocol due to the solubility of the phosphonium ligands synthesised.

Cationic phosphonium gold nanoparticles dispersed in DMSO

In order to prepare the colloidal gold nanoparticles in DMSO, solutions of the phosphonium ligands, triphenylphosphoniopropylthiosulfate zwitterion, (3-thioacetylpropyl)triphenylphosphonium bromide and tri(*p*-tolyl)phosphoniopropylthiosulfate zwitterion were prepared in DMSO (0.25 mmol, 0.30 mmol, and 0.8 mmol respectively). The volume used for these solutions was 20 mL. A solution of potassium tetrachloroaurate (0.12 mmol) in DMSO (10mL) was also prepared. Then both, ligand and gold salt solutions were mixed and stirred. The reduction was carried out by adding 5 mL of freshly prepared aqueous

solution of sodium borohydride (2.0 mmol) to the DMSO mixture. In order to remove the excess of ligands in each one of the gold colloidal solutions prepared, liquid-liquid extractions were carried out using diethyl ether.

Cationic phosphonium gold nanoparticles dispersed in water

Solutions of the phosphonium ligands (triphenylphosphoniopropylthiosulfate zwitterion and (3-thioacetylpropyl)triphenylphosphonium bromide) was prepared in 20 mL of dichloromethane (DCM) (0.25 mmol, 0.30 mmol, 0.8 mmol respectively) and potassium tetrachloroaurate (0.12 mmol) was also added to the DCM solution.[35,36] This was vigorously stirred for 2 hours and until the potassium gold salt was totally dissolved. The reduction of the gold (III) to gold (0) in the presence of phosphonium ligand was carried out by adding drop by drop a freshly prepared sodium borohydride solution in water (3ml, 400 mM) with vigorous stirring. After 20 minutes of stirring, 15 mL of deionised water was then added to the mixture. The latter is kept stirring overnight. The initial DCM was removed from the aqueous phase, as the functionalised nanoparticles transferred to this phase. Then, three liquid-liquid extractions were carried out using DCM in order to purify the cationic phosphonium gold nanoparticles dispersed in water.

3. Results and Discussion

(a) Synthesis of tri(*p*-tolyl)phosphoniopropylthiosulfate zwitterion

The synthesis of the tri(*p*-tolyl)phosphoniopropylthiosulfate zwitterion involved the preparation of two intermediates, which were obtained and purified in order to get the zwitterion. The first compound synthesised was the hydroxylpropylphosphonium salt and this was obtained by the quaternisation of the tri(*p*-tolyl)phosphine with bromopropanol as it is showed in Scheme 1. The hydroxypropyl-tri(*p*-tolyl)phosphonium bromide was then treated

with HBr in order to obtain the ω-bromopropyl-tri(*p*-tolyl)phosphonium bromide. The latter is then reacted with $Na_2S_2O_3$ in aqueous ethanol. The resulting zwitterion was purified by trituration using diethyl ether. The final product had an oil appearance, yellow coloured. When studied by ESMS in positive ion mode, ion corresponding to $M+H^+$ was observed (459). The ^1H NMR showed the distinctive chemical shift at 2.3 corresponding to the nine protons from the $–CH_3$ attached to the aromatic ring. This chemical shift is the main difference between the tri(*p*-tolyl)phosphoniopropylthiosulfate and the triphenylphosphoniopropylthiosulfate ^1H NMR spectra. It can be assumed that the sulfur-sulfur bond of both tri(*p*-tolyl)phosphoniopropylthiosulfate undergoes cleavage with the loss of the sulfite ion under reductive conditions as in the synthesis of gold colloidal nanoparticles, as it was shown and reported in the case of the triphenylphosphoniopropylthiosulfate. This cleavage will allow the sulfur of the cationic phosphonium ligand to interact with the gold nanoparticle surface. As previously mentioned, these thiosulfate and thioacetate ligands are usually known as masked thiol ligands. For triphenylphosphoniopropylthiosulfate zwitterion and (3-thioacetylpropyl)triphenylphosphonium bromide, similar results to the previously reported were observed when studied by IR, NMR and ESI-MS. Solubility tests were carried out to all three masked thiol ligands. They were soluble in methanol, ethanol, DMSO, chloroform and DCM.

(b) Cationic phosphonium gold nanoparticles dispersed in DMSO and water

The triphenylphosphoniopropyl thiosulfate and (3-thioacetylpropyl)triphenylphosphonium bromide ligands have shown their ability to functionalised and stabilised gold nanoparticles surface in water. For this work, another biocompatible solvent, DMSO, was used in order to assist with the solubilisation of more hydrophobic ligand (in our case the tri(*p*-

tolyl)phosphoniopropyl thiosulfate zwitterion), its interaction with gold nanoparticle surface, and then penetration into the lipophilic cell wall. These thiosulfate containing salts are also known as Bunte salts. Shon et al. were the first in showing the production of alkanethiolate-gold nanoparticles from Bunte salts.[37] They used sodium S-dodecylthiosulfate and showed that the sulfur-sulfur bond of the thiosulfate salt undergoes cleavage and acted as the free thiol.[35,37] Functionalised gold nanoparticles dispersed in water were obtained when triphenylphosphoniopropylthiosulfate and (3-thioacetylpropyl)triphenylphosphonium bromide ligands, and the two-phase liquid-liquid (DCM/water) method were used. However, when tri(*p*-tolyl)phosphoniopropylthiosulfate zwitterion was used as the protecting ligand with the same method, no transfer of these nanoparticles to the water phase was observed, and, therefore, no stable gold colloidal nanoparticles were obtained in water. Various attempts of synthesising phosphonium cationic gold nanoparticles were carried out using tri(*p*-tolyl)phosphoniopropylthiosulfate zwitterion as the stabilising ligand and the two phase DCM/water method. Concentration of this ligand was also increased to a double (80 mM) and same results were obtained. Therefore, in the case of the tri(*p*-tolyl)phosphoniopropyl thiosulfate zwitterion, even increments in the concentration of the ligand did not help to the formation functionalised gold nanoparticles dispersed in water using the *p*-tolyl ligand.

DMSO was chosen as an alternative solvent to disperse the gold nanoparticles functionalised with tri(*p*-tolyl)phosphoniopropylthiolate ligand. Due to the properties described in the introduction, DMSO was used to synthesise gold nanoparticle functionalised with the tri(*p*-tolyl)phosphoniopropylthiosulfate zwitterion, and also be able to use more hydrophobic phosphonium ligands to fabricate carriers with potential abilities to permeate and penetrate the lipophilic cell walls.

In order to prepare the colloidal gold nanoparticles in DMSO, a reduction of gold (III) to gold (0) was carried out in the presence of tri(*p*-tolyl)phosphoniopropylthiosulfate zwitterion in

DMSO, using sodium borohydride as the reducing agent. With this reducing method using DMSO as the dispersing solvent, a ruby – coloured colloidal solution of gold nanoparticle functionalised with tri(*p*-tolyl)phosphoniopropylthiolate was obtained. Using the same method in DMSO, other colloidal solutions of gold nanoparticles functionalised using triphenylphosphoniopropylthiosulfate zwitterion and (3-thioactylpropyl)triphenylphosphonium bromide as protecting ligands were also successfully obtained. Stability studies were also carried out in order to monitor over time the potential aggregation in the colloidal solutions prepared following this method.

(c) UV-Visible and TEM studies

Using UV-Vis spectroscopy technique, formation of colloidal gold nanoparticles in DMSO (Figure 1) and as previously mentioned, stability of these solutions were monitored (Figures 2 to 4).

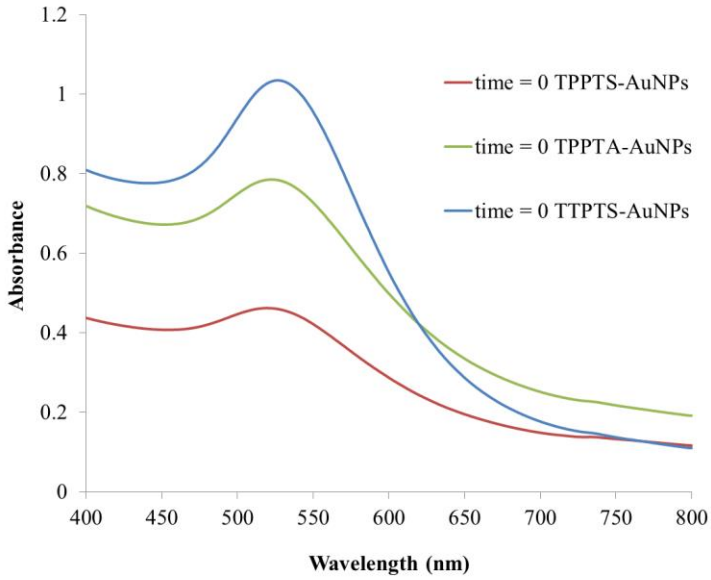

Figure 1. UV-visible absorption spectra of the colloidal solutions of gold nanoparticles functionalised with triphylphosphoniopropylthiosulfate zwitterion (TPPTS-AuNPs), (3-thioacetylpropyl)triphenylphosphonium bromide (TPPTA-AuNPs), and tri(*p*-tolyl)phosphoniopropylthiosulfate zwitterion (TTPTS-AuNPs) in DMSO, time = 0.

It is well-known that the dark-red colour of gold colloids dispersed in water reflects the surface plasmon band (SPB), which is a broad absorption band in the visible region around 520 nm.[38] The SPB is due to the collective oscillations of the electrons at the surface of nanoparticles (6s electrons of the conduction band for AuNPs) that is correlated with the electromagnetic field of the incoming light.[39] The maximum and bandwidth are also influenced by the particle size.[40-43] It has been shown that for gold nanoparticles of mean diameter of 9, 15, 22, 48, and 99 nm, the SPB maximum λ_{max} was observed at 517, 520, 521, 533, and 575 nm, respectively, in aqueous media.[40,44]

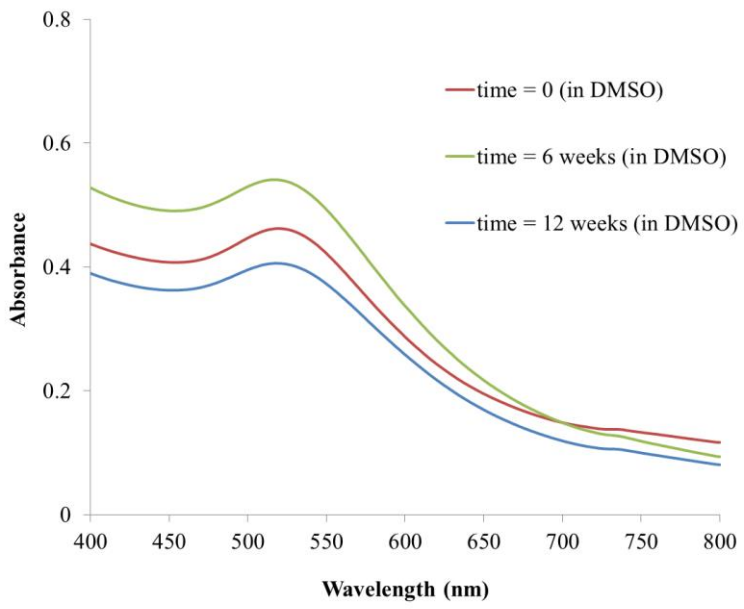

Figure 2. UV-visible absorption spectra of the colloidal solutions of gold nanoparticles functionalised using triphylphosphoniopropylthiosulfate zwitterion as protecting ligand (TPPTS-AuNPs). The different UV-visible spectra represent these nanoparticles dispersed in DMSO at time = 0, 6 and 12 weeks.

The method for the synthesis of colloidal gold nanoparticles in DMSO using triphenyl- and tri(*p*-tolyl)phosphoniopropylthiolate as protecting ligands is reported for the first time in this work. Evidence of the formation of gold nanoparticles using the reduction method in DMSO was shown by UV-Visible spectroscopy technique. Using the DMSO as the blank, bands centred at 519, 519 and 529 nm were observed in the resulting UV spectra (Figure 1) corresponding to the burgundy gold colloidal solutions prepared with triphenylphosphoniopropylthiosulfate (TPPTS-AuNPs), (3-thioacetylpropyl)triphenylphosphonium bromide (TPPTA-AuNPs) and tri(*p*-tolyl)phosphoniopropylthiosulfate (TTPTS-AuNPs), respectively. Their stability was also monitored by UV-Vis spectroscopy and the DMSO solutions showed to be stable at least for 12 weeks (Figures 2, 3 and 4). The colloidal solutions were stored in the dark and at room temperature.

As previously reported and repeated for this work for comparison purposes, [35,36,45] gold nanoparticles synthesised using triphenylphosphoniopropylthiosulfate and (3-thioacetylpropyl)triphenylphosphonium bromide as protecting ligands, dispersed in water showed broad bands centred at 519 nm in both cases in the UV-visible spectra. When compared the UV spectra of the colloidal solutions of gold nanoparticles functionalised with triphenylphosphoniopropylthiolate in water and DMSO (time = 0), they did not show significant differences in the wavelengths. In our case the refractive index of the solvent DMSO has not shown to induce a shift of the SPB of our nanoparticles as suggested in the literature.[44]

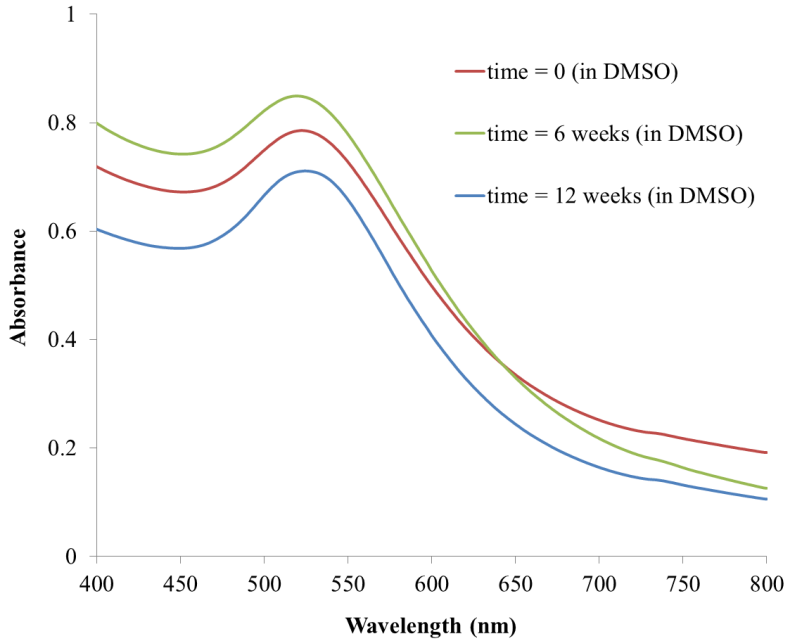

Figure 3. UV-visible absorption spectra of the colloidal solutions of gold nanoparticles functionalised using (3-thioacetylpropyl)triphenylphosphonium bromide as protecting ligand (TPPTA-AuNPs). The different UV-visible spectra represent these nanoparticles dispersed in DMSO at time = 0, 6 and 12 weeks.

It is known that the ligand shell also alters the refractive index and causes either a red or blue shift.[41] This shift is especially significant with thiolate ligands, which are responsible for a strong ligand field interacting with surface electron cloud.[41] Similar evidence can be observed when compared the colloidal solutions in DMSO of gold nanoparticles stabilised with triphenylphosphoniopropylthiolate ligand with the one corresponding to gold nanoparticles functionalised with tri(*p*-tolyl)phosphoniopropylthiolate. Differences in wavelengths (519 and 529 nm, respectively) can be observed when ligands change in structure (see Figures 2 and 4).

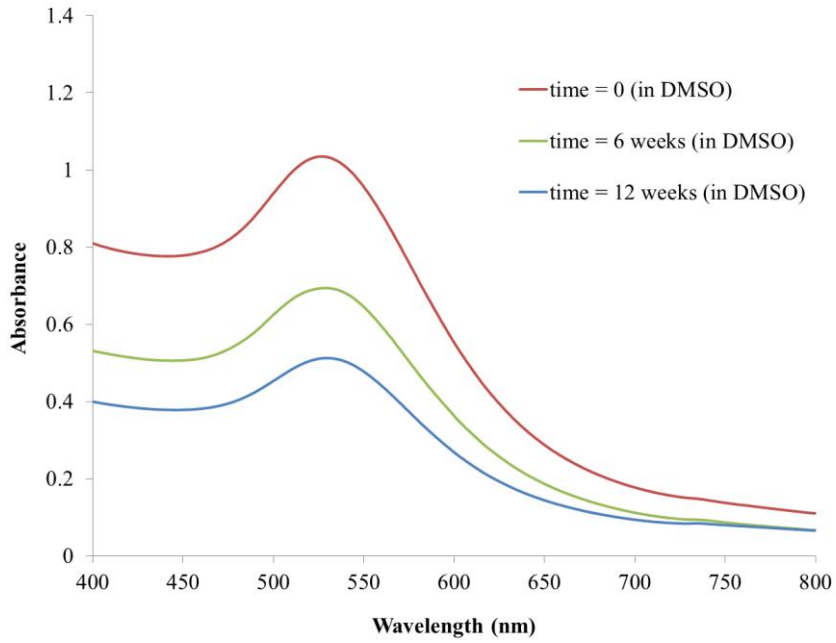

Figure 4. UV-visible absorption spectra of the colloidal solutions of gold nanoparticles functionalised using tri(*p*-tolyl)phosphoniopropylthiosulfate zwitterion as protecting ligand (TTPTS-AuNPs). The different UV-visible spectra represent these nanoparticles dispersed in DMSO at time = 0, 6 and 12 weeks.

The colloidal solutions of gold nanoparticles functionalised using triphenylphosphoniopropyl thiosulfate (Figure 5, **TEM1**), (3-thioacetylpropyl)triphenylphosphonium bromide (Figure 5, **TEM2**) and tri(*p*-tolyl)phosphoniopropylthiosulfate (Figure 5, **TEM3**) as protecting ligands, were all analysed by TEM. Micrographs of all three gold nanoparticle samples showed spherical or semi-spherical shaped particles. Then, particle sizes for samples **TEM1**, **TEM2** and **TEM3** were obtained by analysing at least 150 particles per sample from several images taken.

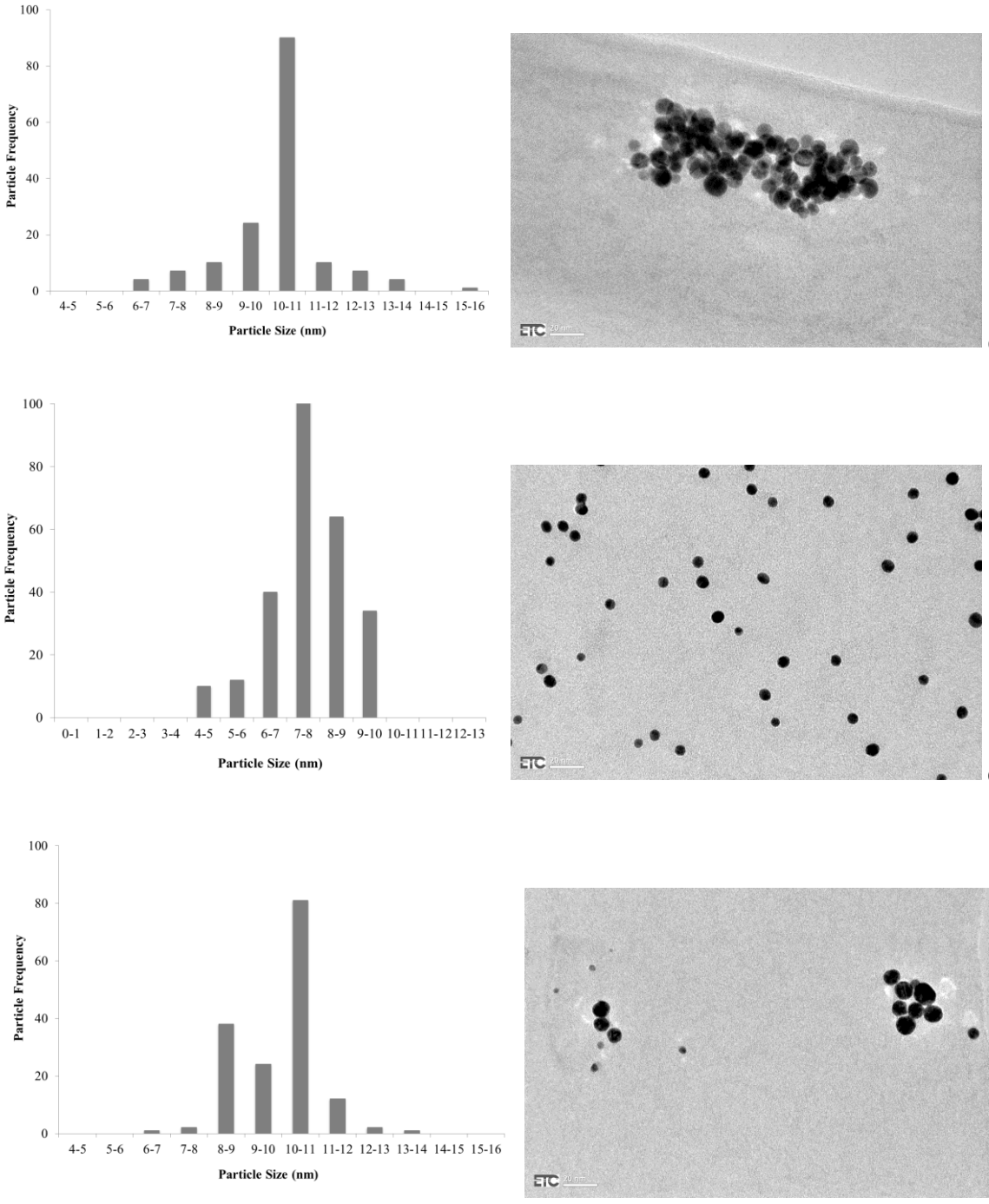

Figure 5. Representative TEM micrographs of cationic phosphonium gold nanoparticles synthesised using triphenylphosphoniopropylthiosulfate **(TEM1)**, (3-thioacetylpropyl)triphenylphosphonium bromide **(TEM2)**, and tri(*p*-tolyl)phosphoniopropylthiosulfate **(TEM3)** as protecting ligands in DMSO, and corresponding particle size histograms.

All samples showed similar in particle sizes, and the mean values were obtained by calculating the averages and standard deviations. The calculated mean diameters were the followings: 11 ± 1 nm (**TEM1**), 8 ± 1 nm (**TEM2**) and 10 ± 1 nm (**TEM3**). Samples TEM1 and TEM2 showed similar particle sizes to ones reported and synthesised using the two-phase DCM/water method.[35,36] These evidences are confirmed by the ones found in the corresponding UV-Visible spectra. Although, solvents used to disperse the nanoparticles were different, the principle of the reduction method used and also the concentrations used for both methods, two phase DCM/water and DMSO, were similar.

Gold nanoparticles in DMSO derived from triphenylphosphoniopropylthiosulfate zwitterion, and (3-thioacetylpropyl)triphenylphosphonium bromide are slightly different in size and in particle size distribution. This can be due to the differing passivation kinetics of the types of ligands used for this study, and the cleavage of the sulfur-sulfur and sulfur-carbon bonds in the thiosulfate and thioacetate species.[45] The mechanisms of these cleavages are still unclear. However, the presence of water traces in the solvent used for the synthesis of colloidal gold nanoparticles, has shown to be crucial for the hydrolysis of the thiosulfate and thioacetate ligands and formation of alkylthiolates.[46,47] These thiolate anions will lead to the formation of phosphonium-functionalised gold nanoparticles. The presence of reducing agent in the solution also influences the cleavage of sulfur-sulfur and sulfur-carbon bonds.[45]

In the case of the tri(*p*-tolyl)phosphoniopropylthiolate functionalised gold nanoparticles, they could only be produced using the DMSO method. The corresponding UV-Visible spectrum showed that the SPB is centred at 529 nm (Figure 4). With this evidence only, it could have been assumed that nanoparticles were slightly larger in size than the ones functionalised with the triphenylphosphoniopropylthiolate ligands, which showed bands centred at 519 nm (Figures 2 and 3). The slight blue shift observed in the UV-Visible spectrum of the tri(*p*-tolyl)phosphoniopropylthiolate functionalised gold nanoparticles might be due to the ligand

shell altering the refractive index and interacting more strongly with the electron cloud of the nanoparticle surface, and not to the particle size. This evidence supports Su et al. experimental observations and results.[41]

The agglomeration of nanoparticles can be observed in TEM1 and TEM3 micrographs (Figure 5). This recurrent experimental observation can be due to the use of drop deposition method for sample preparation. This technique is widely used for TEM sample preparation, however, according to studies reported in the literature,[48] the use of this method can lead to agglomeration of particles at the substrate edges as the solvent evaporates. This accumulation will also depend on the sample concentration. No particle agglomeration can be observed in the case of gold nanoparticles prepared using (3-thioacetylpropyl)triphenylphosphonium bromide (TEM2, Figure 5). We can speculate that in this case, the sample concentration was lower than in the case of the solutions of gold nanoparticles prepared with the other two ligands.

4. Conclusions

The fabrication of cationic phosphonium gold nanoparticles using triphenylphosphoniopropylthiosulfate zwitterion, (3-thioacetylpropyl)triphenylphosphonium bromide and tri(*p*-tolyl)phosphoniopropylthiosulfate zwitterion as protecting ligands and a reduction method in DMSO is reported here for the first time; and also the synthesis of a new masked thiol, tri(*p*-tolyl)phosphoniopropylthiosulfate zwitterion. These Bunte salts and thioacetate ligands offer an advantage over the free thiol ligands as they showed better stability to air oxidation. The use of a biocompatible solvent such as DMSO to produce these nanoparticles can represent an advantage for their potential applications as novel therapeutic agents, especially, when more hydrophobic ligands (in our case, tri(*p*-tolyl)phosphoniopropylthiosulfate zwitterion) are used to functionalised gold nanoparticles,

as they may have more affinity with the lipophilic cell walls. We have shown that under reductive conditions in DMSO, the formation of these nanoparticles occurred in the presence of all three cationic phosphonium ligands synthesised for this work. We have shown that the thiosulfate and thioacetate compounds convert into the corresponding thiolate anions. We can assume that these anions interact with the surface of the gold nanoparticles produced *in situ* when strong reducing agent is added to the DMSO solutions. The formation and the stability over time of triphenylphosphoniopropylthiolate and tri(*p*-tolyl)phosphoniopropylthiolate functionalised gold nanoparticles in DMSO were confirmed and followed by UV-visible spectroscopy. Bands centred at 519 and 529 nm, respectively, were observed in the UV-visible spectra, and those did not change over a period of 3 months. We can also speculate that the changes in the ligands chemical structure can affect the refractive index of the colloidal solution and produce a shift to the left (blue shift). As previously mentioned, tri(*p*-tolyl)phosphoniopropylthiolate functionalised gold nanoparticles were successfully produced and dispersed in DMSO, however, these nanoparticles could not be obtained using the two-phase liquid/liquid (DCM/water) method and dispersed in water. The TEM analyses of cationic phosphonium gold nanoparticles functionalised using triphenylphosphoniopropylthiosulfate and tri(*p*-tolyl)phosphoniopropylthiosulfate zwitterions as protecting ligands, showed similar particle sizes (11 nm). However, when (3-thioacetylpropyl)triphenylphosphonium bromide used, the size of nanoparticles obtained was different (8 nm). This might be due to different passivation kinetics of the thiosulfate and thioacetate containing ligands.

Visualisation of the cellular internalisation of our lipophilic cationic moieties containing gold nanoparticles by using flow cytometry technique is planned for future. This is a biophysical technique usually employed in the diagnosis of various health disorders. The cells are normally suspended in a stream of fluid and passed them by and electronic detection

apparatus. In order to prepare the samples for cytometry analysis, our cationic phosphonium gold nanoparticles are planned to be internalised by incubation.

5. Characterisation of the cationic phosphonium ligands

Hydroxypropyl-tri(p-tolyl)phosphonium bromide

IR spectrum showed absorption bands at the regions of 725–720 cm^{-1} (ν CH_2), 1600cm^{-1} (ν C-O), 3100–3000 cm^{-1}(ν CH-Aromatic), and 3344 cm^{-1} (ν C-OH) . ^{1}H NMR spectrum gave signals at δ 1.8 (9H,s $2CH_3$) , δ 2.0 (2H,m, -CH_2-), δ 2.6 (1H,s, OH), δ 3.4 (2H,m, P-CH_2), δ 3.6 (2H,t, OH-CH_2) , and δ 7.3-7.5 (12H,m, Aromatic H) ppm. ESI-MS 363 [M - Br], 364 [M – Br] +[H^+].

ω-bromopropyl-tri(p-tolyl)phosphonium bromide

IR spectrum showed absorption bands at the regions of 677cm^{-1} (ν C-Br), 748 cm^{-1} (ν CH_2), 988 cm^{-1} (ν P-CH_2), and 3100–3000 cm^{-1}(ν CH-Aromatic). ^{1}H NMR spectrum gave signals at δ 2.3 (9H,s, -CH_3) , δ 2.4(2H,m, P-CH_2) , δ 3.8 (2H,m, -CH_2-) and at 7.4- 7.9 (12H,m, Aromatic H) ppm. ESI-MS 427 [M].

Tri(p-tolyl)phosphoniopropylthiosulfate zwitterion

IR spectrum showed absorption bands at the regions of 725–720 cm^{-1}, (ν CH_2), 1329cm^{-1} (ν S=O), 1400 cm^{-1} (ν C-S), 3100–3000 cm^{-1} (ν CH-Aromatic). ^{1}H NMR showed a signals at δ 2.3 (s,9H, $3CH_3$) , δ 3.2 (t, 2H , P-$\underline{CH_2}$-CH_2-CH_2) , δ 3.4 (t, 2H , P -CH_2-CH_2-$\underline{CH_2}$) , δ 3.6 (m, 2H , P-CH_2-$\underline{CH_2}$-CH_2), δ 7.24 (1H , $CDCL_3$), and δ 7.3-7.6 (12H,m, Aromatic H) ppm. ESI-MS 459 [M + H^+].

Triphenylphosphoniopropylthiosulfate zwitterion

IR spectrum showed absorption bands at the regions IR spectrum showed absorption bands at the regions of 725–720 cm^{-1} (ν CH_2), 1330 cm^1 (ν S=O), 1345 cm^{-1} (C-S-), and 3100–3000 cm^{-1} (ν CH-Aromatic). ^{1}H NMR spectrum gave signals at δ 2.2 (2H,m, P-$\underline{CH_2}$-CH_2-CH_2) , δ 3.3 (2H,m, P-CH_2-CH_2-$\underline{CH_2}$) , δ 4.0 (2H,m, P-CH_2-$\underline{CH_2}$-CH_2) and at 7.6 - 7.8 (15H,m, Aromatic H) ppm. ESI-MS 417 [M + H^+].

(3-Thioacetylpropyl)triphenylphosphonium bromide

IR spectrum showed absorption bands at the regions of 735–740 cm^{-1} (ν CH_2), 1345 cm^{-1} (ν C-S), 1470–1450 cm^{-1} (ν C–H corresponding to bend-CH_2), 1678 cm^{-1} (ν C=O), and 3100–3000 cm^{-1}(ν CH-Aromatic). ^{1}H NMR showed a signals at δ 2.4 (3H,s, -CH_3), δ 2.9 (2H,m, P-$\underline{CH_2}$-CH_2-CH_2), δ 3.8 (2H,m, P-CH_2-CH_2-$\underline{CH_2}$), δ 4.1 (2H,m, P-CH_2-$\underline{CH_2}$-CH_2), and δ 7.6-7.9 (15H,m, Aromatic H) ppm. ESI-MS 380 [M + H^+].

Acknowledgements

We would like to thank the Libyan Embassy for funding Wanisa's PhD project and also to Ashley Howkins (ETC, Brunel University London) for the provision of the TEM micrographs.

References

1 M. Ferrari, *Nat. Rev., Cancer*, 2005, **5**, 161-171.

2 G.F. Paciotti, L. D.G.I. Kingston, L. Tamarkin, *Drug Dev. Res.*, 2006, **67**, 47-54.

3 G.Y. Tonga, D.F. Moyano, C.S. Kim, V.M. Rotello, *Curr. Op. Coll. & Int. Sci.*, 2014, **19**, 49-55.

4 N.L. Rosi, C.A. Mirkin, *Chem. Rev*., 2005, **105**, 1547-1562.

5 M.M.C. Cheng, G. Cuda, Y.L. Bunimovich, M. Gaspari, J.R. Heath, H.D. Hill, C.A. Mirkin, A.J. Nijdam, R. Terracciano, T. Thundat, M. Ferrari, *Curr. Op. Chem. Biol*., 2006, **10**, 11-19.

6 K. Saha, S.S. Agasti, C. Kim, X. Li, and V.M. Rotello, *Chem. Rev*., 2012, **112**, 2739-2779.

7 P. Ghosh, G. Han, M. De, C.K. Kim, V.M. Rotello, *Adv. Drug Deliv. Rev*., 2008, **60**, 1307-1315.

8 A. Schroeder, D.A. Heller, M.M. Winslow, J.E. Dahlman, G.W. Pratt, R. Langer, T. Jacks, D.G. Anderson, *Nat. Rev. Cancer*, 2012, **12**, 39-50.

9 T.M. Allen, P.R. Cullis, *Science*, 2004, **303**, 1818-1822.

10 M.R. Dreher, W. Liu, C.R. Michelich, M.W. Dewhirst, F. Yuan, A. Chilkoti, *J. Natl. Cancer Inst.*, 2006, **98**, 335-344.

11 H. Maeda, J. Wu, T. Sawa, Y. Matsumura, K. Hori, *J. Control. Release*, 2000, **65**, 271-284.

12 R.M. Sawant, J.P. Hurley, S. Salmaso, A. Kale, E. Tolcheva, T.S. Levchenko, V.P. Torchilin, *Bioconjug. Chem*., 2006, **17**, 943-949.

13 E.C. Cho, Q. Zhang, Y.N. Xia, *Nat. Nanotechnol*., 2011, **6**, 385-391.

14 C.S. Kim, B. Duncan, B. Creran, V.M. Rotello, *Nano Today*, 2013, **8**, 439-447.

15 E.C. Cho, L. Au, Q. Zhang, Y.N. Xia, *Nano Lett*. 2009, **9**, 1080-1084.

16 E.C. Cho, L. Au, Q. Zhang, Y.N. Xia, *Small*, 2010, **6**, 517-522.

17 J. Dausend, A. Musyanovych, M. Dass, P. Walther, H. Schrezenmeier, K. Landfester, V. Mainlander, *Macromol. Biosci*., 2008, **8**, 1135-1143.

18 H. Yang, S.Y. fung, M.Y. Liu, *Angew. Chem. Int. Ed*., 2011, **50**, 9643-9646.

19 E. Oh, J.B. Delehanty, K.E. Sapsford, K. Susumu, R. Goswami, J.B. Banco-Canosa, P.E. Dawson, J. Granek, M. Shoff, Q. Zhag, P.L. Goering, A. Huston, I.L. Medintz, *ACS Nano*, 2011, **5**, 6434-6448.

20 N.A. Al-Hajaj, A Moquin, K.D. Neibert, G.M. Soliman, F.M. Winnik, D. Maysinger, *ACS Nano*, 2001, **5**, 4909-4918.

21 N. Zhan, G. Palui, M. Safi, X. Ji, H. Mattoussi, *J. Am. Chem. Soc*., 2013, **135**, 13786-13795.

22 Z.J. Zhu, Y.C. Yeh, R. Tang, B. Yan, J. Tamayo, W. Vachet, V.M. Rotello, *Nat. Chem*., 2011, **3**, 963-968.

23 B. Ballou, B.C. Lagerholm, L.A. Ernst, P.M. Bruchez, A.S. Waggoner, *Bioconj. Chem*., 2004, **15**, 79-86.

24 Y. He, Y. Zhong, Y. Su, Y. Lu, Z. Jiang, F. Peng, T. Xu, S. Su, Q. Huang, C. Fan, S.T. Lee, *Angew. Chem. Int. Ed.*, 2011, **50**, 5695-5698.

25 B. Dubertret, P. Skourides, D.J. Norris, V. Noireaux, A.H. Brivanlou, A. Libchaber, *Science*, 2002, **298**, 1759-1762.

26 K. Saha, D.F. Moyano, V.M. Rotello, *Mater. Horiz*., 2014, **1**, 102-105.

27 C.M. McIntosh, E.A. Esposito, A.K. Boal, J.M. Simard, C.T. Martin, V.M. Rotello, *J. Am. Chem. Soc*., 2001, **123**, 7626-7629.

28 M.P. Murphy, R.J.A. Smith, *Annu. Rev. Pharmacol. Toxicol*., 2007, **47**, 629-656.

29 M.F. Ross, T. Da Ros, F.H. Blaikie, T.A. Prime, C.M. Porteous, I.I. Severina, V.P. Skulachev, H.G. Kjaergaard, R.A.J. Smith, M.P. Murphy, *Biochem. J.*, 2006, **400**, 199-208.

30 M.F. Ross, G.F. Kelso, F.H. Blaikie, A.M. James, H.M. Cocheme, A. Filipovska, T. Da Ros, T.R. Hurd, R.A.J. Smith, M.P. Murphy, *Biochemistry (Moscow)*, 2005, **70**, 222-230.

31 C.N.R. Rao, S.R.C. Vivekchand, K. Biswas, A. Govindaraj, *Dalton Trans.*, 2007, **34**, 3728-3749.

32 W.H. Binder, R. Sachsenhofer, C.J. Straif, R. Zirbs, *J. Mater. Chem*., 2007, **17**, 2125-2132.

33 S. Pyrpassopoulos, D. Niarchos, G. Nounesis, N. Boukos, I. Zafiropoulou, V.

Tzitizioe, *Nanotechnology*, 2007, **18**, 485604.

34 http://www.accessdata.fda.gov/cms_ia/importalert_169.html (accessed date: 01/10/2014)

35 Y. Ju-Nam, N. Bricklebank, D.W. Allen, P.H.E. Gardiner, M.E. Light, M.B. Hursthouse, *Org. Biomol. Chem*., 2006, **4**, 4345–4351.

36 Y. Ju-Nam, D.W. Allen, P.H.E. Gardiner, N. Bricklebank, *J. Organomet. Chem.*, 2008, **693**, 3504–3508.

37 Y.S. Shon, S.M. Gross, B. Dawson, M. Porter, R.W. Murray, *Langmuir*, 2000, **16**, 6555-6561.

38 A.P. Alivisatos, *Science*, 1996, **271**, 933-937.

39 D.L. Feldheim, and A.F. Colby, *Metal Nanoparticles-Synthesis, Characterization and Applications*, Jr., Eds., Marcel Dekker, New York, 2002.

40 S. Link, M.A. El-Sayed, *J. Phys. Chem. B*, 1999, 103, 4212-4217.

41 K.H Su, Q.H. Wei, X. Zhang, J.J. Mock, D. Smith, S. Schulz, *Nano Lett*., 2003, **3**, 1087-1090.

42 S. Link, M.B. Mohamed, M.A. El-Sayed, *J. Phys. Chem. B*, 1999, **13**, 3073-3077.

43 B. Yan, Y. Yang, Y. Wang, *J. Phys. Chem. B*, 2003, **107**, 9159-9159.

44 M. C. Daniel, D. Astruc, *Chem. Rev.*, 2004, **104**, 293-346.

45 Y. Ju-Nam, Y-S. Chen, J.J. Ojeda, D.W. Allen, N.A. Cross, P.H.E. Gardiner, N. Bricklebank, *RSC Adv.*, 2012, **2**, 10345-10351.

46 R.J. Fealy, S.R. Ackerman, and G.S. Ferguson, *Langmuir*, 2011, **27**, 5371-5376.

47 R.G. Pillai and M.S. Freund, *Langmuir*, 2011, **27**, 9028-9033.

48 K.J. Wilkinson, and J.R. Lead, *Environmental Colloids and Particles: Behaviour, Separation and Characterisation*, Eds., John Wiley and Sons, Chichester, 2007.